AGU PUBLICATIONS

JGR

Journal of Geophysical Research: Oceans

RESEARCH ARTICLE

10.1002/2013JC009514

Key Points:
- Inorganic carbon concentration increase in intermediate water layers of the Arctic Ocean
- No significant trend in nutrient or oxygen concentrations was found
- Inflow of anthropogenic carbon to intermediate layers is the likely cause

Correspondence to:
L. G. Anderson,
leifand@chem.gu.se

Citation:
Ericson, Y., A. Ulfsbo, S. van Heuven, G. Kattner, and L. G. Anderson (2014), Increasing carbon inventory of the intermediate layers of the Arctic Ocean, *J. Geophys. Res. Oceans*, *119*, 2312–2326, doi:10.1002/2013JC009514.

Received 21 OCT 2013
Accepted 15 MAR 2014
Accepted article online 20 MAR 2014
Published online 14 APR 2014

Increasing carbon inventory of the intermediate layers of the Arctic Ocean

Ylva Ericson[1], Adam Ulfsbo[1], Steven van Heuven[2], Gerhard Kattner[3], and Leif G. Anderson[1]

[1]Department of Chemistry and Molecular Biology, University of Gothenburg, Gothenburg, Sweden, [2]Centre for Isotope Research, University of Groningen, Groningen, Netherlands, [3]Alfred-Wegener-Institut Helmholtz-Zentrum für Polar und Meeresforschung, Bremerhaven, Germany

Abstract Concentrations of dissolved inorganic carbon (DIC), total alkalinity (TA), nutrients, and oxygen in subsurface waters of the central Arctic Ocean have been investigated for conceivable time trends over the last two decades. Data from six cruises (1991–2011) that cover the Nansen, Amundsen, and Makarov Basins were included in this analysis. In waters deeper than 2000 m, no statistically significant trend could be observed for DIC, TA, phosphate, or nitrate, but a small rate of increase in apparent oxygen utilization (AOU) was noticeable. For the individual stations, differences in concentration of each property were computed between the mean concentrations in the Arctic Atlantic Water (AAW) or the upper Polar Deep Water (uPDW), i.e., between about 150 and 1400 m depth, and in the deep water (assumed invariable over time). In these shallower water layers, we observe significant above-zero time trends for DIC, in the range of 0.6–0.9 μmol kg^{-1} yr^{-1} (for AAW) and 0.4–0.6 μmol kg^{-1} yr^{-1} (for uPDW). No time trend in nutrients could be observed, indicating no change in the rate of organic matter mineralization within this depth range. Consequently, the buildup of DIC is attributed to increasing concentrations of anthropogenic carbon in the waters flowing into these depth layers of the Arctic Ocean. The resulting rate of increase of the column inventory of anthropogenic CO_2 is estimated to be between 0.6 and 0.9 mol C m^{-2} yr^{-1}, with distinct differences between basins.

1. Introduction

The impact on climate, by accelerating fossil fuel burning, is mitigated by oceanic CO_2 uptake and storage [e.g., *Ballantyne et al.*, 2012]. Roughly 25% of the present annual anthropogenic CO_2 (C_{ant}) emissions are stored in the oceans [e.g., *Le Quéré et al.*, 2009]. However, as a consequence of the resulting decrease of the oceanic buffer capacity [*Revelle*, 1983], this fraction will decline with time and there are already signs of a reduced absorption rate in several oceanic regions [e.g., *Schuster et al.*, 2009; *Lenton et al.*, 2012]. Despite its remoteness, the Arctic Ocean not only plays an integral role in the global heat balance, but it also contains nearly 2 times the global mean concentration of anthropogenic CO_2 [*Tanhua et al.*, 2009], a feature related to the intense ventilation of subsurface layers.

In the Arctic Ocean, the renewal of Atlantic layer, intermediate, and deep Arctic waters is driven by: (i) inflow of Atlantic water through Fram Strait, (ii) Atlantic water that crosses over the Barents Sea where it cools down, and (iii) dense water formation by brine released during sea ice production, especially in polynyas along the Arctic shelf seas [*Rudels et al.*, 2012a], with subsequent descent of high-salinity bottom waters down the continental slope [*Anderson et al.*, 1999]. Cooling of the inflowing surface waters increases gas solubility and thus promotes uptake of CO_2 from the atmosphere. Furthermore, brine production has been suggested to facilitate uptake of CO_2 from the atmosphere both by promoting water transport from the surface to the deep [e.g., *Anderson et al.*, 2004; *Omar et al.*, 2005; *Else et al.*, 2011] as well as by calcium carbonate formation in the brine channels that changes the pCO_2 levels in both the brine and the sea ice melt [*Rysgaard et al.*, 2011]. The ventilation of the subsurface waters transports C_{ant} to the deep ocean. Downward transport of C_{ant} may be further enhanced by the hypothesized increasing strength of the biological pump [e.g., *Riebesell et al.*, 2007]. The Atlantic layer and intermediate water masses of the Arctic Ocean flow in an cyclonic pattern along topographic boundaries before exiting through Fram Strait and, beyond that, over the Scotland-Greenland Ridge to the Atlantic Ocean thereby linking the Arctic to the global thermohaline circulation [e.g., *Mauritzen*, 1996; *Anderson et al.*, 1999].

The rate of warming of the Arctic atmosphere exceeds the global mean [*Serreze and Francis*, 2006] and coincides with a significant decrease of summer sea ice extent and volume [e.g., *Stroeve et al.*, 2007, 2012; *Laxon*

Table 1. List of Cruises, International Arctic Ocean Expedition 1991 (IAOE 91), Arctic Ocean Section 1994 (IAS 94), Arctic Climate System Study 1996 (ACSYS 96), Beringia 2005, Trans-Arctic Survey of the Arctic Ocean in Transition (TransArc) From Which the C-System Data Were Collected

Survey (Vessel)	Date	Parameters	Source (doi)	Comment
IAOE 91 (I/B Oden)	26 Jul 1991 to 3 Sep 1991	S, T, O_2, DIC*, TA*, nutrients	10.3334/CDIAC/otg. CARINA_77DN19910726	*No CRMs. CARINA data product
AOS 94 (I/B L. St Laurent)	24 Jul 1994 to 1 Sep 1994	S, T, O_2, DIC, TA, nutrients	10.3334/CDIAC/otg. CARINA_18SN19940724	CARINA data product
ACSYS 96 (R/V Polarstern)	Jul 12 1996 to 6 Sep 1996	S, T, O_2, DIC, TA, pH, nutrients	10.3334/CDIAC/otg. CARINA_06AQ19960712	CARINA data product
Beringia 2005 (I/B Oden)	19 Aug 2005 to 25 Sep 2005	S, T, O_2, DIC, TA, pH, nutrients	10.3334/CDIAC/otg. CLIVAR_77DN20050819	
ARK-XXII/2(R/V Polarstern)	28 Jul 2007 to 10 Oct 2007	S, T, O_2*, DIC, TA, nutrients		*Calibrated CTD-oxygen
TransArc/ARK-XXVI/3 (R/V Polarstern)	5 Aug 2011 to 7 Oct 2011	S, T, O_2*, DIC, TA, pH, nutrients	doi.pangaea.de/10.1594/ PANGAEA.775817	*Calibrated CTD-oxygen

et al., 2013]. The presence of sea ice restricts further sea ice growth through its insulating effect. More open water thus facilitates increased sea ice production and brine formation during the winter season, with the prospect of increased deep water formation adding to the surface-to-deep ocean anthropogenic carbon transport [*Anderson et al*., 2004; *Else et al*., 2011]. On the other hand, excessive heat in the inflowing Atlantic water is likely to have the opposite impact in previously seasonally ice-covered areas like the Barents Sea [*Harms*, 1997; *Årthun et al*., 2011].

More open water in the Arctic Ocean also allows for a substantial uptake of atmospheric CO_2 because of less impediment of air-sea gas exchange [*Bates and Mathis*, 2009; *Jutterström and Anderson*, 2010]. Such changes in sea ice conditions, together with rising temperature and the effects thereof on stratification, mixing, and upwelling, are likely to affect primary production [*Tremblay and Gagnon*, 2009]. To what magnitude is not currently possible to conclude, because the changes of these processes could act both negatively and positively. Satellite monitoring suggests that net primary production (NPP) has increased by 20% between 1998 and 2009, largely as a result of the shrinking sea ice cover [*Arrigo and van Dijken*, 2011; *Arrigo et al*., 2011]. Whether this increased productivity will enhance the biological pump remains uncertain. Nevertheless, sea ice-related shifts in Arctic ecosystems are likely to alter carbon fluxes to subsurface layers [*Li et al*., 2009]. Lastly, there is a potential for more production by, and sedimentation of, sea ice algae because more first-year sea ice will lead to better light and thus growth conditions [*Boetius et al*., 2013]. Important unknowns are the amount of the organic matter that sinks and the depth at which it remineralizes.

Historic observations of nutrients in the central Arctic Ocean show very constant concentrations from about 2000 m to the bottom of around 14 μmol kg^{-1} in nitrate and 1 μmol kg^{-1} in phosphate [e.g., *Codispoti et al*., 2013]. Observations of oxygen and dissolved inorganic carbon (DIC) also show very constant concentrations with depth, but below an even shallower depth for the latter. Together with the very low organic matter content of sediments [e.g., *Jakobsson et al*., 2003] and the long residence times of the bottom water (hundreds of years) [e.g., *Tanhua et al*., 2009; *Rudels et al*., 2012a], this strongly supports the notion that the rate of organic carbon export to below 2000 m is very low.

In order to assess conceivable changes in DIC concentrations in subsurface waters of the Arctic Ocean resulting from anthropogenic CO_2 uptake and alterations in the biological carbon pump during the last decades when the sea ice concentration and thickness have decreased, we evaluate the evolution of measured concentrations of the carbon system, oxygen, and nutrients.

2. Methods

2.1. Data Provenance

The cruises during which the data were collected are listed in Table 1, and their station locations are presented in Figure 1. The data from the 1990s are included in the Arctic Ocean data compilation [*Jutterström et al*., 2010] within the carbon dioxide in the Atlantic Ocean (CARINA) data synthesis project [*Key et al*., 2010]. Table 2 provides a detailed description of station positions and data availability. Properties

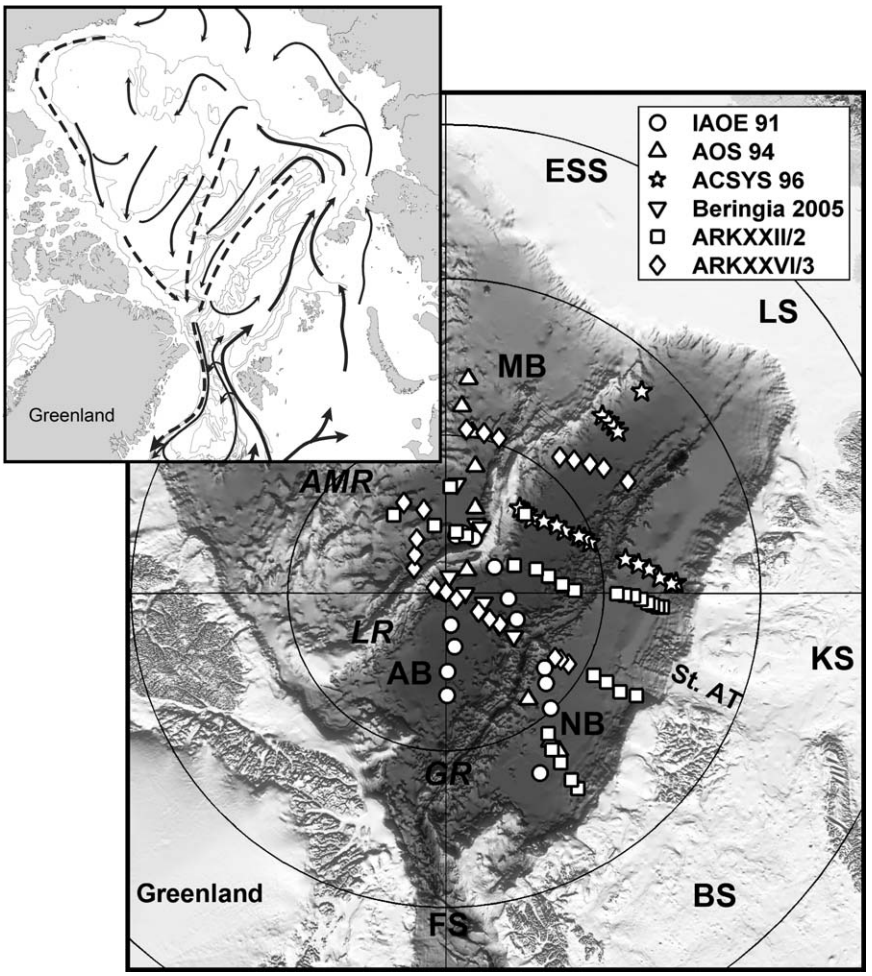

Figure 1. Map of the Arctic Ocean with station locations for carbon system data and an insert showing the main circulation pattern. The abbreviations note the basins, Nansen (NB), Amundsen (AB), Makarov (MB), and Canada (CB), the three ridges, Alpha-Mendeleev (*AMR*), Lomonosov (*LR*), and Gakkel (*GR*) as well as Fram Strait (FS), Barents Sea (BS), Kara Sea (KS), Laptev Sea (LS), and East Siberian Sea (ESS). St. Anna trough is denoted as St. AT.

considered in this contribution are DIC, total alkalinity (TA), pH, oxygen (expressed as apparent oxygen utilization, AOU), nutrients (phosphate and nitrate), all from discrete water samples, and temperature and salinity from the conductivity-temperature-depth (CTD) records.

During all cruises, DIC was determined using coulometric titration according to *Johnson et al*. [1987], following the standard operating procedure outlined in *Dickson et al*. [2007]. The precision (here reported as the standard deviation of differences between duplicate sample runs, except for the Beringia 2005 and ARK-XXVI/3 cruises where the precision is reported as the mean absolute difference) was 1–2 μmol kg^{-1} for all but the ARK-XXVI/3 cruise, which had a precision of 4 μmol kg^{-1}. TA was determined by open cell potentiometric titration according to *Haraldsson et al*. [1997] and, for ARK-XXII/2, *Mintrop et al*. [2000], except for the IAOE 91 cruise where a closed cell potentiometric titration was used [*Johansson and Wedborg*, 1982]. The precision was ~2 μmol kg^{-1} for all but the IAOE 91, which had a precision of 4 μmol kg^{-1}. For both DIC and TA determinations, the accuracy was assured by the use of Certified Reference Materials (CRM) supplied by A. Dickson, Scripps Institution of Oceanography (USA), with the exception for the IAOE 91 cruise during which CRM was not yet available. A spectrophotometric method was used for the pH determination [*Clayton and Byrne*, 1993], with a precision around 0.001 pH units. The total pH scale is used throughout this work. Oxygen was determined with automated Winkler titration systems, with a relative precision of better than 1%. During the 2007 and 2011 TransArc cruises oxygen are from an oxygen sensor mounted on the CTD package, with the data calibrated by Winkler titrations. Thus, the precision should be comparable to

Table 2. Year and Positions of the Stations as Well as Parameters Used in This Evaluation[a]

Year	Stn	Latitude (°N)	Longitude (°E)	DIC	TA	O_2	NUT
1991	5	83.56	27.63	*	*	*	*
1991	9	85.07	42.30	*	*	*	*
1991	10	85.73	48.05	*		*	*
1991	11	86.07	52.79	*	*	*	*
1991	16	87.61	69.70	[b]	[b]	[b]	[b]
1991	17	88.01	85.06		[c]	*	*
1991	19	88.25	118.50	*	*	*	*
1991	25	88.04	152.81			*	*
1991	26	88.02	163.60		*	*	*
1991	27	88.16	169.69		*	*	*
1991	29	90	0		*	*	*
1991	30	88.99	8.94	*	*	*	*
1991	31	88.28	9.34	*	*	*	*
1991	32	87.51	1.44		*	*	*
1991	33	86.76	0.75	*	*	*	*
1994	25	83.173	173.935	*	*	*	*
1994	26	84.063	175.072	*	*	*	*
1994	27	84.852	170.693	*	*	*	*
1994	28	85.892	166.703	*	*	*	*
1994	29	87.155	160.708	*	*	*	*
1994	34	89.017	137.152	*	*	*	*
1994	35	89.998	66.992	*	*	*	*
1994	36	85.733	37.748	*	*	*	*
1994	37	84.245	35.008	*	*	*	*
1994	38	83.845	35.690	*	*	*	*
1996	38	82.68	92.52	*	[d]	*	*
1996	39	82.84	92.32			*	*
1996	40	83.20	94.04	*	[d]	*	*
1996	41	83.50	96.58	*	[d]	*	*
1996	42	83.83	98.40	*	[d]	*	*
1996	43	84.20	100.53	*	[d]	*	*
1996	50	85.17	109.29			*	*
1996	51	85.28	111.59	*	[d]	*	*
1996	52	85.41	113.01	*	[d]	*	*
1996	54	85.76	117.47			*	*
1996	55	85.88	121.24	*	[d]	*	*
1996	56	86.15	125.95		*	*	*
1996	57	86.40	130.63	[c]	[c]	*	*
1996	58	86.39	134.19		*	*	*
1996	59	86.43	136.04	*	*	*	*
1996	60	86.44	138.89	[d]	*	*	*
1996	79	82.50	138.47			*	*
1996	80	82.50	136.41	*	*	*	*
1996	81	82.50	134.61			*	*
1996	82	82.52	132.95	*	*	*	*
1996	87	81.08	135.69	*	[d]	*	*
2005	26	86.538	174.153	*	*	*	*
2005	30	87.614	156.073	*	*	*	*
2005	31	87.640	151.610	*	*	*	*
2005	42	89.473	167.492	*	*	*	*
2005	44	89.380	89.087	*	*	*	*
2005	46	88.762	75.128	*	*	*	*
2005	47	88.045	58.437	*	*	*	*
2005	49	87.444	57.686	*	*	*	*
2007	255	82.503	33.952			*	*
2007	256	82.858	33.877			*	*
2007	257	83.498	34.043	*	*	*	*
2007	258	83.999	34.014	[b]	*	*	*
2007	260	84.489	36.139	[e]	[e]	*	*
2007	261	84.645	60.934	*	*	*	*
2007	263	84.172	60.998			*	*
2007	264	83.642	60.429			*	*
2007	266	83.138	61.741	[f]	*	*	*
2007	294	83.115	86.246			*	*
2007	295	83.272	86.284	*	*	*	*
2007	296	83.435	86.746			*	*
2007	297	83.588	87.237			*	*
2007	298	83.807	88.098	*		*	*

Table 2. (continued)

Year	Stn	Latitude (°N)	Longitude (°E)	DIC	TA	O_2	NUT
2007	299	84.051	89.043	*	*	*	*
2007	300	84.337	89.292			*	*
2007	301	84.580	89.837	g	*	*	*
2007	306	85.923	91.122	*	*	*	*
2007	307	86.303	94.287			*	*
2007	308	86.706	99.283			*	*
2007	309	87.046	104.79			*	*
2007	310	87.658	112.04	*	*	*	*
2007	324	88.075	160.63			*	*
2007	326	88.028	170.08	*	*	*	*
2007	328	87.830	189.44	*	*	*	*
2007	333	87.028	213.60	f	f	*	*
2007	352	86.638	177.56	b	b	*	*
2007	363	86.459	135.02	f	f	*	*
2011	201	85.509	59.885	d		*	*
2011	202	85.803	59.932	d		*	*
2011	203	85.974	59.423	d		*	*
2011	212	88.018	59.952	d	*	*	*
2011	213	88.385	59.138			*	f
2011	214	88.794	60.215	d	*	*	*
2011	216	89.600	60.746	d	*	*	*
2011	218	89.964	146.631	d	*	*	*
2011	219	89.615	−115.228	d	*	*	*
2011	222	88.736	−128.249	d	*	*	*
2011	223	88.452	−141.171	d	*	*	*
2011	224	88.060	−152.054	d	*		*
2011	226	87.284	−165.269	d	*	*	*
2011	227	86.861	−155.045	d	*	*	*
2011	244	84.779	172.747	d	*	*	*
2011	245	84.795	166.415	d	*	*	*
2011	246	84.814	160.996	d	*	*	*
2011	250	84.385	139.910	d	*	*	*
2011	251	84.154	135.882	d	*	*	*
2011	252	83.879	131.696	d	*	*	*
2011	253	83.626	128.295	d	*	*	*
2011	258	83.237	121.359	d	*	*	*

[a]As denoted by an asterisk, data are available for all water masses.
[b]No measurements within the AAW.
[c]No measurements within the uPDW.
[d]Calculated using CO2SYS version 1.1 [*van Heuven et al.*, 2011] with the carbonate dissociation constants (K_1 and K_2) of *Mehrbach et al.* [1973] as refit by *Dickson and Millero* [1987].
[e]Only measurements within the dAAW.
[f]No measurements within the dAAW.
[g]Only measurements within the uPDW.

the precision of the latter. Nutrients were measured by an autoanalyzer according to standard procedures (e.g., following the World Ocean Circulation Experiment (WOCE) protocol) [*Gordon et al.*, 1994], with a relative precision better than 2%. The nutrients of the ARK-XXVI/3 cruise were converted to μmol kg^{-1} at an assumed analysis temperature of 20°C.

The carbonate system was overdetermined during the ACSYS 96, Beringia 2005, and ARK-XXVI/3 2011 cruises. Within the CARINA data set (see Tables 1 and 2), the alkalinity of the ACSYS 96 cruise was partially calculated from DIC and pH using the carbonate dissociation constants (K_1 and K_2) of *Mehrbach et al.* [1973] as refit by *Dickson and Millero* [1987]. Because of the noisy character of the DIC data from the ARK-XXVI/3 cruise, DIC was additionally computed from TA and pH^{tot} using CO2SYS [*van Heuven et al.*, 2011], with the

Table 3. Water Mass Classification According to *Marnela et al.* [2008], Adapted From *Rudels et al.* [2005]

Arctic Ocean Water Masses	Density Range
Arctic Atlantic Water (AAW)	$27.70 \leq \sigma_0 < 27.97$
dense Arctic Atlantic Water (dAAW)	$27.97 \leq \sigma_0, \sigma_{0.5} < 30.444, \theta > 0$
upper Polar Deep Water (uPDW)	$\sigma_{0.5} < 30.444, \theta \leq 0$

Table 4. The Fitted Slopes, in μmol kg^{-1} yr^{-1}, With Its Fit (R^2) and Significance (p Value) for the Time Period of the Data of Table 5

	DIC			AOU			TA			Phosphate			Nitrate		
	Slope	R^2	p	Slope	R^2	p	Slope	R^2	p	Slope	R^2	p	Slope	R^2	p
NB	0.05	0.034	0.77	0.26	0.969	0.002	0.22	0.475	0.20	−0.0006	0.047	0.72	−0.019	0.429	0.23
AB	0.10	0.027	0.75	0.41	0.885	0.005	0.12	0.133	0.47	−0.0003	0.017	0.80	−0.004	0.008	0.87
MA	−0.32	0.467	0.31	0.35	0.808	0.038	0.38	0.346	0.30	−0.0001	0.002	0.95	−0.023	0.382	0.27

same constants as for the CARINA data set, giving a precision of the computed DIC of 2 μmol kg^{-1}. The average difference between the measured and calculated DIC is 2.3 ± 4.9 μmol kg^{-1}. This small offset is related to the choice of carbonate dissociation constants and the accuracy of the pH and TA measurements. The precision of calculated DIC (2 μmol kg^{-1}) is indeed superior to that of the direct measurements (about 4 μmol kg^{-1}) and for the remainder of this paper we therefore use the calculated DIC of ARK-XXVI/3, without considering the offset of 2.3 μmol kg^{-1}.

2.2. Deep Water Data Consistency

The quality and interconsistency of the Arctic Ocean data within the CARINA data product were evaluated by *Jutterström et al.* [2010]. To further demonstrate the interconsistency of these data sets and the more recent surveys used in the present study, the mean deep water values of the biogeochemical properties (DIC, TA, phosphate, nitrate, and AOU) were regressed against time for each of the three discerned major ocean basins.

2.3. Time Trends in Near-Surface and Intermediate Water Masses

For our assessment of time trends, we discern (from surface to intermediate depth) the Arctic Atlantic Water (AAW), the dense Arctic Atlantic Water (dAAW), and the upper Polar Deep Water (uPDW), according to Table 3.

For each station with a bottom depth of more than 3000 m and at least three measurements below 2000 m, depth-integrated mean concentrations of the properties in the AAW, dAAW, and uPDW were obtained through trapezoidal integration. The density ranges in the water mass classification (Table 3) were used to determine the depth boundaries of the water masses. The integrated inventories were divided by the local water mass height to obtain the concentrations.

Station-specific systematic errors (e.g., minor calibration inaccuracies) are removed by subtracting the mean of the deep water (DW) values from the depth-integrated mean concentrations of the intermediate waters (IW), which also will correct for any analytical biases between cruises. Thus, a difference is obtained for each station and property, expressed as ΔX ($X^{IW}_{mean} - X^{DW}_{mean}$), and for each basin and cruise the average ΔX is calculated. Linear regression analyses were done for the Nansen, Amundsen, and Makarov Basins using these cruise-specific averages. The significance of the time trends was evaluated using Analysis of Variance (ANOVA).

The effects of organic matter remineralization were deduced by assessing trends in the Δ-values of nutrients and AOU. Changes in ΔTA were investigated to see any potential effects of calcium carbonate dissolution. Effects of changes in CO_2 solubility were investigated utilizing the trends in depth-integrated mean values of salinity and potential temperature at the sampling depths.

3. Results and Discussion

3.1. Deep Water Data Consistency

The overarching assumption that there are no trends in the deep waters was tested by fitting strait lines (Table 4) to the mean concentrations of each cruise and basin for the properties below 2000 m (Table 5). The standard errors of the mean of nearly all data are within double the precision of the analytical methods. The exceptions are DIC in the 2005 Makarov Basin data and TA in the 1991 Nansen Basin data. This large error is due to a larger scatter and no significant increase of the concentration with depth. The mean data of DIC, AOU, and phosphate are also plotted versus year in Figure 2. As obvious from the fit (R^2) and significance (p value < 0.05) only the AOU data show any statistically significant trend (0.4 μmol kg^{-1} yr^{-1}). Without any corresponding trend in any of the other parameters it is not possible to ascribe the AOU trend to any biogeochemical process such as remineralization of organic matter that sediment through the water column. This is

Table 5. Mean Concentrations and Standard Errors (SE) in the Deep Waters (>2000 m) of the Nansen Basin (NB), Amundsen Basin (NB), and Makarov Basin (MB) During the Different Years[a]

		DIC		AOU		TA		Phosphate		Nitrate	
Year		Mean	SE	Mean	SE	Mean	SE	Mean	SE	Mean	SE
1991	NB	2154.0	1.2	56.7	1.0	2295.2	3.4	0.98	0.006	14.7	0.04
	AB	2153.1	1.4	52.9	0.4	2293.0	1.8	0.98	0.003	14.7	0.04
	MA	a	a	60.2	0.5	2290.5	1.0	0.99	0.001	14.9	0.04
1994	NB	2159.4	0.3	57.3	0.1	2297.5	1.3	1.03	0.009	14.5	0.02
	AB	2163.6	0.7	57.2	0.0	2301.3	0.1	1.02	0.001	14.5	0.04
	MA	2159.8	1.0	64.6	0.2	2301.5	0.9	1.04	0.004	14.5	0.01
1996	NB	2155.9	1.4	57.7	0.2	2292.6	1.6	0.97	0.004	14.5	0.05
	AB	2151.2	1.3	57.8	0.1	2294.8	1.7	0.99	0.007	13.7	0.07
	MA	nd	nd	nd	nd	nd	nd	nd	nd	nd	nd
2005	NB	nd	nd	nd	nd	nd	nd	nd	nd	nd	nd
	AB	2162.2	1.9	60.3	0.1	2295.5	0.7	1.02	0.004	14.6	0.08
	MA	2160.7	3.5	67.3	0.3	2305.9	1.0	1.04	0.005	14.8	0.07
2007	NB	2155.0	1.0	60.1	0.2	2297.5	0.9	1.00	0.002	14.6	0.06
	AB	2155.3	1.3	60.2	0.1	2297.9	0.7	1.00	0.001	14.5	0.08
	MA	2154.3	0.8	65.7	0.3	2299.9	0.5	1.02	0.004	14.6	0.06
2011	NB	2158.1	0.6	62.3	0.0	2300.1	0.6	0.97	0.003	14.0	0.07
	AB	2157.0	0.4	63.2	0.2	2299.6	0.3	0.97	0.005	14.1	0.04
	MA	2154.3	0.3	69.3	0.3	2300.6	0.3	0.99	0.007	14.1	0.03

[a]All data are in μmol kg^{-1}. nd: No samples were collected. a: too few samples for a statistical treatment.

also supported by estimates of very low export fluxes of organic matter [*Anderson et al.*, 2003; *Cai et al.*, 2010]. Furthermore, the lack of a significant trend in TA in the deep waters (as well as in the intermediate waters) leads us to conclude that temporal variability in the dissolution of calcium carbonates is insignificant and it therefore will not be considered in the assessment. The intermediate waters are supersaturated with respect to both calcite and aragonite while the deep water is slightly supersaturated for calcite but undersaturated for aragonite [*Jutterström and Anderson*, 2005]. The very low burial of carbonates in the sediment indicates little sedimentation of calcium carbonate.

Even if there is no trend in the DIC, TA, and nutrient data there is a substantial scatter in the mean data between cruises, especially for DIC up to 10 μmol kg^{-1}. As the residence times of these deep waters are long, up to hundreds of years [*Tanhua et al.*, 2009; *Rudels et al.*, 2012a], the combined data sets suggest that biogeochemical variability is a highly unlikely cause of the scatter. However, to further test the importance of organic matter decay as reason for the scatter between cruises, the DIC concentration was corrected by the variability in the AOU, phosphate, and nitrate concentrations. For this correction preformed concentrations were assumed and the RKR ratio of 1:16:106:138 for P, N, C, O_2 was used [*Redfield et al.*, 1963]. The absolute value selected as preformed concentrations are not important in investigating if the scatter in DIC will decrease by this correction, as long as the preformed concentration is constant over time. The resulting corrected DIC showed a very similar concentration range between the years (9–13 μmol kg^{-1}) but with a slightly shift to lower values during the later years when AOU was used. The latter is a natural result based on the significant temporal trend of these data. Hence, this further supports that the DIC scatter between cruises is not due to biogeochemical processes.

Data from deeper than 2500 m of the cruises in the years 1991, 1994, and 1996 have been analyzed for offsets using multilinear regression [*Jutterström et al.*, 2010]. Except for the TA of the 1994 cruise no statistical significant interconsistency in the data set could be detected that warranted an adjustment of the original data. It should be noted that during this analysis the ratios of P, N, and O_2 were allowed to vary (without any biochemical constrains) to get the least variability between the data of the different cruises. The data of the cruises in years 2005, 2007, and 2011 have not been investigated in a corresponding manner. The lack of any temporal trend in the data consistent with biogeochemical processes, together with minimal ocean mixing based on the long residence time, supports the assumption of constant concentrations in the deep water for the analysis of the intermediate water properties.

3.2. Time Trends in Near-Surface and Intermediate Water Masses

Figure 3 and Table 6 summarize the changes (relative to those of the deep water) in the Atlantic layers and the uPDW of the Arctic Ocean, for the time period between 1991 and 2011. For DIC, a significant trend is

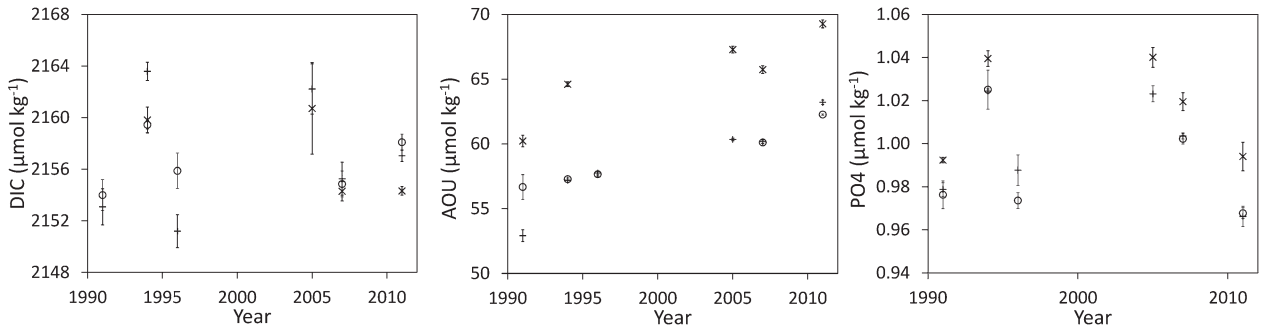

Figure 2. Deep water (≥2000 m) cruise averages (μmol kg^{-1}) including standard error bars within the Nansen (circle), Amundsen (plus), and Makarov (cross) Basins over the period of 1991–2011: (a) DIC, (b) AOU, (c) PO_4.

observed of 0.7–0.9 μmol kg^{-1} yr^{-1} ($p < 0.05$) within the Amundsen Basin (Table 6). The trend becomes less pronounced with depth. Changes within the Nansen and Makarov Basins are 0.6 μmol kg^{-1} yr^{-1} ($p < 0.05$, except for the dAAW of the Makarov Basin) in the Atlantic layers and roughly one third less in the uPDW. The changes in the dAAW and uPDW of the Makarov Basin are not significant (ANOVA, $p > 0.05$) due to the sparse data set and should be interpreted with caution.

The uncertainty in the rate of change of DIC in the different basins and water masses, expressed as the standard errors of the fits, ranges from 0.1 to 0.2 μmol kg^{-1} yr^{-1}, with the largest errors related to the Makarov Basin. The large spread of the DIC data of the IAOE 91 cruise within the Amundsen Basin (Figure 3b) contributes strongly to the uncertainty of the trends. If the IAOE 91 cruise is excluded from the regressions, the corresponding slopes are in the range of 0.6–0.9 μmol kg^{-1} yr^{-1} (ANOVA, $p < 0.05$). These trends are used in the further discussion.

Additional uncertainties may be related to the spatial representativeness of the computed averages, i.e., sample locations within the basin. However, the variation in ΔX is largely within the analytical error. For example, the standard deviation of ΔDIC for each combination of cruise, basin, and water mass is within ±4 μmol kg^{-1} for 89% of the combinations. We therefore assume that the general scarcity of data do not significantly impact the spatial representativeness of the different cruises.

The observation of increasing DIC in all three basins may be accounted for by several processes, including increasing remineralization of inorganic and organic carbon sinking through the water column, changes in water mass circulation, and the degree of CO_2 saturation and input of anthropogenic CO_2 in the inflowing water, each of which will be discussed in the following sections. However, as for the deep waters, no trend in TA was observed in the near-surface and intermediate water masses ruling out dissolution of mineral carbonates. However, as these waters are supersaturated with respect to both calcite and aragonite this is not expected and hence, this process is not considered in the following discussion.

3.3. Attribution of Trends

3.3.1. Organic Matter Mineralization

Changes in the sedimentation and subsequent mineralization of organic matter would be reflected in changes of DIC, nutrients, and oxygen that are proportional to the elemental composition of organic matter [*Redfield et al.*, 1963], and may in principle be inferred from changes in these ancillary properties. However, the oxygen and nutrient content of local waters is additionally dependent on variability of the large-scale circulation. Fortunately, the general circulation pattern within the Arctic Ocean results in a horizontally homogenous concentration field minimizing the potential influence of this effect. No interannual trend is detected in either PO_4 (Figures 3j–3l) or NO_3 (Figures 3m–3o) in the intermediate waters that could account for the significant increases in DIC. On the contrary, there is a small but significant decline in NO_3 and PO_4 in the dAAW of the Amundsen Basin (ANOVA, $p < 0.05$; Table 6). This indicates a minimal temporal trend in remineralization of organic matter over the time period of this study (provided that the residence time has not changed, as we assume here). Furthermore, there was no trend in AOU in any of the basins (Figures 3g–3i). The trend in deep water AOU does imply an equal trend in the shallower water masses. However, organic matter is typically

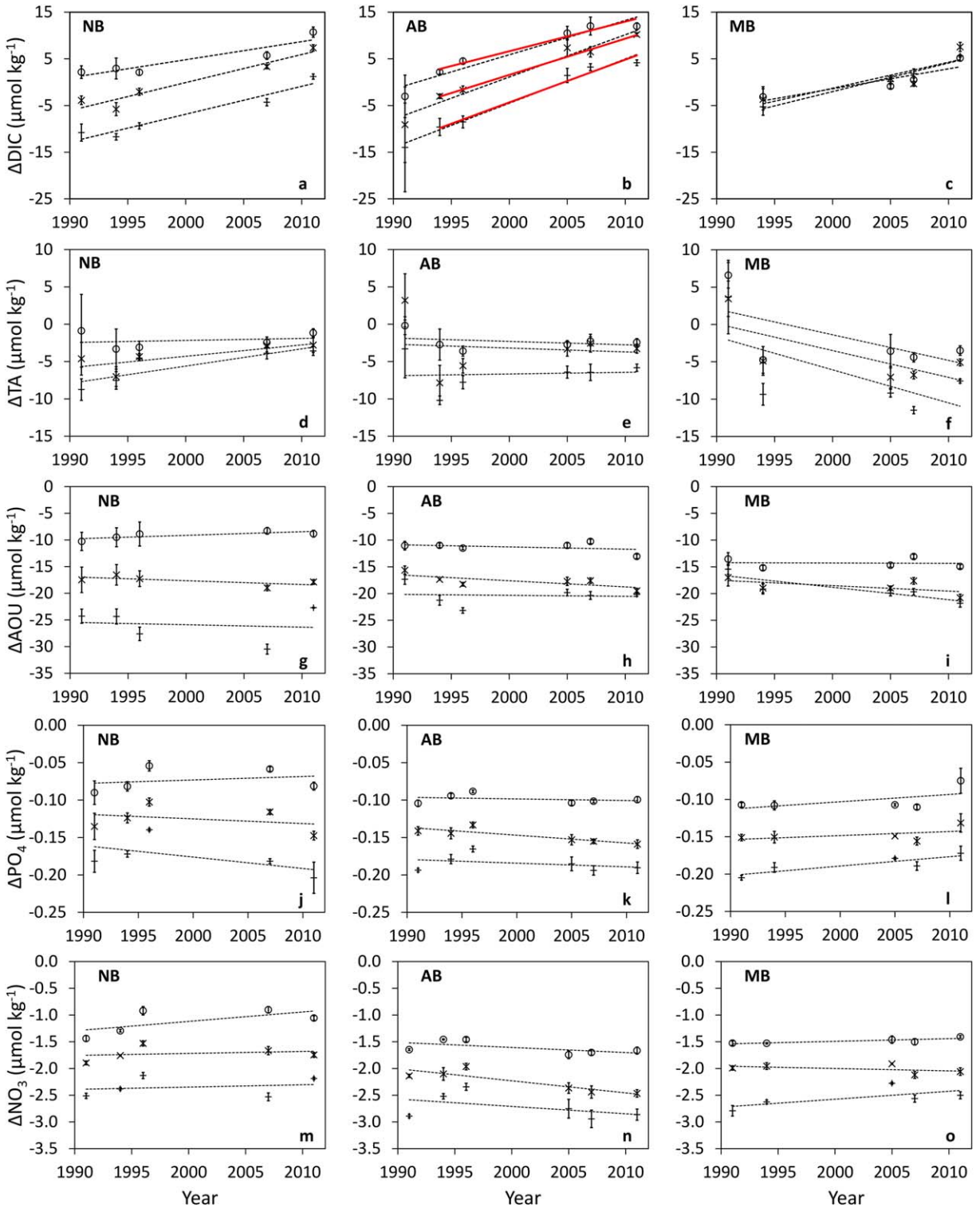

Figure 3. Average ΔDIC, ΔTA, ΔAOU, ΔPO_4, and ΔNO_3 over the period of 1991–2011 including standard error bars for the AAW (plus), dAAW (cross), and uPDW (circle) in the Nansen, Amundsen, and Makarov Basins. The red solid line in (b) is a fit without the 1991 data. Slope coefficient, standard error, *p* values, and R^2 for the different regression lines are displayed in Table 4.

remineralized all through the water column, resulting in a stronger increase of the decay products in the shallower waters compared to the deep. Because no sign of this can be seen in any property, we consider that organic matter mineralization is not a likely cause of the deep water trend in AOU.

Table 6. Slope Coefficients With Standard Error of the Fits, Significance (*p* Value) and R^2 Values[a]

	Nansen Basin				Amundsen Basin				Makarov Basin			
	Slope	SE	p	R^2	Slope	SE	p	R^2	Slope	SE	p	R^2
AAW												
ΔDIC	0.60	0.10	0.01	0.93	0.90 (0.95)	0.09 (0.07)	0.00 (0.00)	0.97 (0.98)	0.61	0.08	0.02	0.97
ΔTA	0.23	0.08	0.06	0.74	0.02	0.14	0.88	0.01	−0.44	0.31	0.25	0.41
ΔAOU	−0.05	0.21	0.84	0.02	−0.02	0.12	0.89	0.01	−0.23	0.08	0.06	0.75
ΔPO_4	−0.0015	0.0013	0.32	0.33	−0.0005	0.0006	0.48	0.13	0.0013	0.0004	0.06	0.76
ΔNO_3	0.004	0.012	0.74	0.04	−0.014	0.013	0.35	0.22	0.015	0.009	0.20	0.47
dAAW												
ΔDIC	0.60	0.10	0.01	0.93	0.79 (0.91)	0.07 (0.09)	0.00 (0.00)	0.98 (0.96)	0.56	0.24	0.14	0.74
ΔTA	0.15	0.07	0.13	0.59	−0.05	0.23	0.83	0.01	−0.36	0.20	0.17	0.52
ΔAOU	−0.07	0.04	0.20	0.47	−0.12	0.05	0.09	0.55	−0.10	0.08	0.28	0.37
ΔPO_4	−0.0006	0.0011	0.61	0.10	−0.0010	0.0003	0.03	0.75	0.0005	0.0005	0.39	0.25
ΔNO_3	0.004	0.009	0.69	0.06	−0.023	0.006	0.02	0.78	−0.004	0.005	0.43	0.22
uPDW												
ΔDIC	0.39	0.10	0.03	0.79	0.61 (0.74)	0.08 (0.10)	0.01 (0.00)	0.95 (0.93)	0.43	0.16	0.11	0.79
ΔTA	0.03	0.07	0.73	0.04	−0.04	0.07	0.54	0.10	−0.34	0.25	0.27	0.38
ΔAOU	0.07	0.03	0.11	0.62	−0.04	0.05	0.48	0.13	−0.01	0.06	0.92	0.00
ΔPO_4	0.0005	0.0010	0.68	0.07	−0.0002	0.0004	0.59	0.08	0.0010	0.0008	0.32	0.32
ΔNO_3	0.018	0.012	0.24	0.42	−0.009	0.006	0.19	0.38	0.005	0.002	0.07	0.72

[a]DIC values for the Amundsen Basin are given without the 1991 data and with the 1991 data in parentheses.

3.3.2. CO_2 Solubility Changes

The variability in depth-integrated mean values of potential temperature and salinity is displayed in Figure 4. The AAW has become warmer and saltier since 1991. This warming has been noted in several previous contributions [e.g., *Schauer et al.*, 2002; *Polyakov et al.*, 2010; *Korhonen et al.*, 2012]. Pulses of inflowing warm Atlantic water have been proposed to cause this increase [*Rudels et al.*, 2013]. A warming of 0.5°C reduces DIC by roughly 3 μmol kg^{-1} due to the decrease in CO_2 solubility (assuming that the water was in prolonged contact with the atmosphere during warming). Such an effect could come about in the source waters during their transit along the Norwegian coast and through the Barents Sea when they are in contact with the atmosphere. The limited decadal variability in temperature and salinity of all water masses but the AAW in the Nansen Basin (Figure 4) results in CO_2 solubility changes that are well below the standard error of the computed trends in inorganic carbon.

3.3.3. Anthropogenic CO_2

The magnitude and spatial distribution of the inorganic carbon changes in the central Arctic Ocean between 1991 and 2011 are thus most likely a result of the increasing C_{ant} in the source waters before leaving contact with the atmosphere. This statement is based on the absence of concomitant changes in either solubility or the mineralization rate of organic matter over the same period. The increase in the integrated column inventory over the Atlantic and intermediate layers of the Amundsen Basin is 0.9 ± 0.1 mol C m^{-2} yr^{-1}. This is nearly two thirds more than the global ocean's rate of increase of the column inventory of C_{ant} [*Sabine et al.*, 2008] and can be compared to inventory increases of 0.6 ± 0.1 mol C m^{-2} yr^{-1} in the Nansen and Makarov Basins. Estimates of the C_{ant} concentration using the transit time distribution together with the CFC distribution also showed the highest column inventory at this depth range in the Amundsen Basin [*Tanhua et al.*, 2009].

As a result of the increases in DIC, together with a constant TA, the pH is reduced by 0.02–0.05 units during the last two decades (starting at about 8.05–8.06 units). This lowers the aragonite and calcite saturation states by 0.05–0.14 and 0.08–0.22 units, respectively (starting at about 1.2–1.4 and 1.9–2.3, respectively). At such rates, it will take less than 100 years for the water to be undersaturated with respect to aragonite, a process starting in the Atlantic layers of the Amundsen Basin.

3.3.3.1. Source Waters of Anthropogenic CO_2

As the input of C_{ant} occurs at the atmosphere-ocean interface there is a need to describe the formation process of the source waters to the water masses to be assessed. The intermediate waters of the Arctic Ocean have an Atlantic origin, and enter both through Fram Strait and the relatively shallow Barents Sea. The West Spitsbergen Current (WSC) contributes to form the Fram Strait Branch of Atlantic Water (FSBW) that flows to

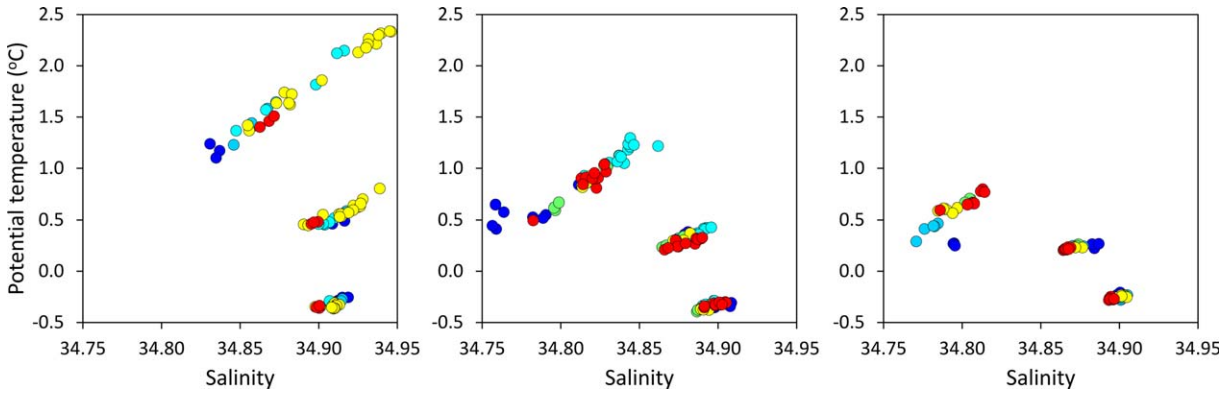

Figure 4. Depth-integrated mean values of potential temperature and salinity for each of the AAW, dAAW, and uPDW at each station in the Nansen Basin (NB), Amundsen Basin (AB), and Makarov Basin (MB), including the 1991 (dark blue), 1994 (blue), 1996 (cyan), 2005 (green), 2007 (yellow), and 2011 (red) cruises.

the east and follows the Barents Sea continental margin. The upper ~100 m melts sea ice and forms cold, low salinity upper water that separates from the warm Atlantic layer water by a strong halocline [e.g., *Rudels et al*., 1996]. At the St. Anna canyon, the FSBW meets the Barents Sea Branch Water (BSBW) and is forced into the deep Nansen Basin.

The conditions of the BSBW are set in the Barents Sea by cooling and some freshening (with sea ice melt) and by mixing with the Norwegian Coastal Current resulting in a large density range. The BSBW contributes to shelf slope convection [*Schauer et al*., 2002], which facilitates efficient surface-to-deep ocean ventilation all from the halocline to about 2000 m depth. In the deep Arctic Ocean, the BSBW flows to the east making it the main source of the intermediate waters of the Amundsen Basin, as well as the Makarov Basin [*Rudels et al*., 2013]. The flow of the BSBW forces the FSBW to turn around north of the Laptev Sea along the south side of the Gakkel Ridge and thereby mainly confines it to the Nansen Basin [e.g., *Jones et al*., 1995; *Rudels et al*., 2013].

The rate of increase of DIC in the surface waters of the Norwegian Atlantic Current (NwAC) at 66°N was 1.3 ± 0.7 μmol kg^{-1} yr^{-1} during the period 2001–2007 [*Skjelvan et al*., 2008]. Correcting for biogeochemical transformation, these authors computed the annual increase of C_{ant} to be ~1 μmol kg^{-1} at 200–400 m depth. Furthermore, *Olsen et al*. [2006] estimated C_{ant} to increase in the West Spitsbergen Current (WSC) at a rate of 0.57–0.67 μmol kg^{-1} yr^{-1} during the time period 1981–2002/2003. The surface water pCO_2 increase in the Barents Sea largely follows the atmospheric record [*Omar et al*., 2003], which means that the C_{ant} concentration increases correspondingly. The atmospheric growth rate of CO_2 at Mount Zeppelin, Ny Ålesund (1993–2012) corresponds to a time trend in DIC of 0.8 μmol kg^{-1} yr^{-1}, as computed for waters with the alkalinity, salinity, and temperature properties of the Amundsen Basin AAW at equilibrium with the atmosphere (Figure 5).

The DIC increases at rates of 0.9 and 0.8 μmol kg^{-1} yr^{-1} within the AAW and dAAW, respectively, in the Amundsen Basin. Considering the uncertainties of these rates (Table 6) they are equal to the C_{ant} growth rate of the Barents Sea (formation region of Amundsen and Makarov Basins waters) and slightly higher than the C_{ant} changes in the WSC (formation region of Nansen Basin waters) estimated by *Olsen et al*. [2006], but smaller than the C_{ant} trends in the NwAC (preformation region of all investigated waters) [*Skjelvan et al*., 2008]. In all other of our investigated water masses, the C_{ant} increase is about the same or less than that of the WSC [*Olsen et al*., 2006].

The changes within the Makarov Basin were in the same range as those in the Nansen Basin, especially within the Atlantic layers. However, the origin of these water masses is more complex than in the Nansen and Amundsen Basins. Waters of different origin with different signatures contribute in unknown proportions to the Atlantic and intermediate layers. This includes water from the Atlantic Ocean that enters over the Lomonosov Ridge and waters from the Pacific Ocean that are modified on the shelf leading to shelf plumes penetrating into different water depths.

3.3.3.2. Relation Between Anthropogenic CO_2 and the Source Water CO_2

Our trends in DIC are of the same size or lower than the increase in C_{ant} of the source waters. How realistic is this in view of the mixing regime of the water masses?

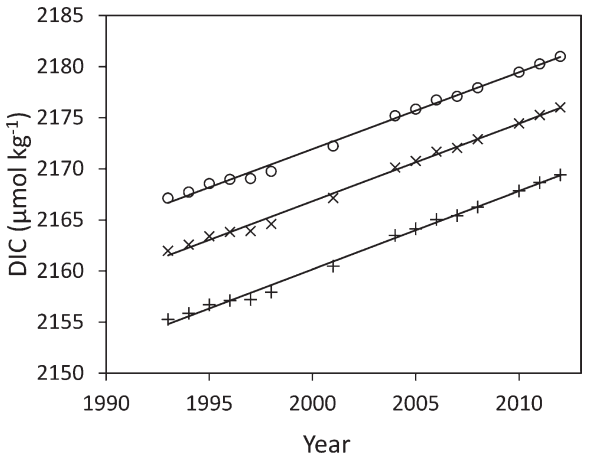

Figure 5. The estimated increase in DIC based on the annual average atmospheric CO_2 content at Mount Zeppelin, Ny Ålesund (Mount Zeppelin, Ny Ålesund, 1989–2012/1993–2012; H.-C. Hansson, personal communication 2013) and average properties of salinity, temperature, TA, phosphate, and silicate, within the AAW (+), dAAW (x), and uPDW (circle) of the Amundsen Basin, using CO2SYS [*van Heuven et al*., 2011]. Slope coefficients, R^2, and *p* values for the different regression lines are for AAW 0.77 μmol kg^{-1} yr^{-1}, 0.995, and 0.00; for dAAW 0.76 μmol kg^{-1} yr^{-1}, 0.995, and 0.00; and for uPDW 0.75 μmol kg^{-1} yr^{-1}, 0.995, and 0.00.

While the boundary current around the Arctic Ocean continental margins and ridges is relatively confined and thus can be represented by a freight train model, horizontal mixing, e.g., by eddies becomes more important toward the basin interior. This means that the evolution of C_{ant} in the inflow regions likely cannot directly represent the evolution in the basins, but rather a realistic model approach has to be taken. Volume transports of the inflowing waters of 2–4 Sv [e.g., *Tsubouchi et al*., 2012] give residence times of around 20 years for the Atlantic layers of the Nansen and Amundsen Basins, with the exact result depending on how much water enters the individual layers and basins. A simple box model illustrates the DIC evolution for a constant rate of C_{ant} increase (corresponding to the atmospheric increase at Ny Ålesund) in the inflowing water (Figure 6). As seen from the model result, the rate of DIC increase in the basin is close to our basin observations but lags by approximately 10–30 years, as seen when comparing the rates of Figures 5 and 6. However, as the rate of increase in atmospheric pCO_2 has been fairly constant for several decades this lag is not relevant for the period of observation. Hence, assuming a corresponding consistent rate of increase in surface water DIC, we conclude that our modeled rate of increase of DIC gives a good approximation of reality.

A further increase in the DIC temporal trend would occur if the ventilation rate has increased during the period of our study. This would be seen in deviations from a straight line in the slope of DIC (Figures 3a–3c). A slight deviation is observed but this is within the data precision.

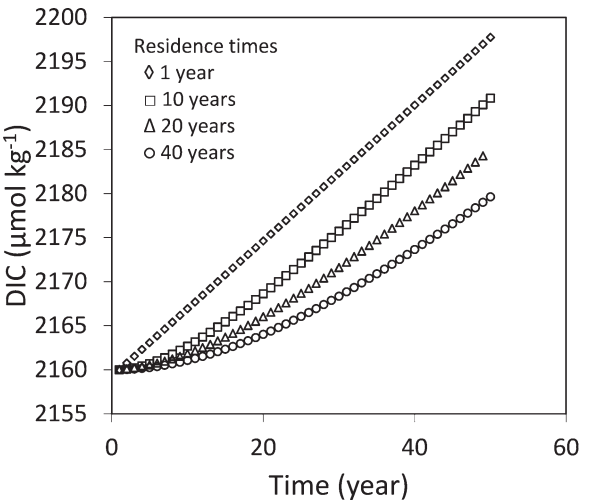

Figure 6. Time evolution of DIC in a simple box model where water of increasing DIC concentration, 0.77 μmol kg^{-1} yr^{-1}, is entering the box. Four different residence times of water in the box is presented.

4. Summary and Conclusions

Observations of DIC in the central Arctic Ocean (Nansen, Amundsen, and Makarov Basins) reveal significant temporal trends in the Atlantic and intermediate layers during the period from 1991 to 2011. The rates of change are between 0.6 and 0.9 μmol kg^{-1} yr^{-1} in the Atlantic layers and between 0.4 and 0.6 μmol kg^{-1} in the uPDW.

The increase in the column inventory of DIC of the Atlantic and intermediate layers is estimated to be between 0.6 and 0.9 mol C m^{-2} yr^{-1} in the different basins. No statistically significant trend is detected in deep water DIC over this time period. Neither is any significant trend detected in nutrients (both phosphate and nitrate) throughout the intermediate water column as well as within the deep water indicating minimal impact by biogeochemical processes. A change in AOU

is found between the cruises in the deep waters, which can, however, not be explained by information available.

If the increase in the AOU data reflects the true situation, the deep waters are not in steady state. Potential reasons for an increase in AOU are either a decrease in the ventilation of the deep waters, an increase in the organic matter sedimentation rate, or an increase in a flux of reduced chemical compounds from the Gakkel Ridge. All but the last should also result in an increase in nutrients and DIC. Changes in the summer sea ice coverage has been suggested to increase primary production and thus potentially also the sedimentation of organic matter. More open water in the fall can also potentially increase brine production leading to ventilation of subsurface waters, but the lowering of salinity by sea ice melt has the opposite effect by stabilizing the water column thus hampering ventilation. However, the change in summer sea ice coverage over the deep central basins is a relatively recent feature and it is highly unlikely that it can contribute to a change starting in the early 1990s. On the other hand, is it well known that deep water formation in the Greenland Sea more or less stopped in the 1990s [e.g., *Rudels et al*., 2012b] and it is also known that the deep waters of the Arctic Ocean is renewed by inflow from the Norwegian Sea [e.g., *Bönisch and Schlosser*, 1995]. These inflowing waters are a mixture of outflowing Arctic Ocean deep waters and Greenland Sea deep water. A decrease in Greenland Sea deep water could result in an increase in AOU of the Arctic Ocean deep water. Further research like thorough data mining with modeling exercise including the Nordic Seas is necessary to test this potential assumption.

Because of lack of time trends in the nutrient concentrations, illustrating absence of changes in mineralization of organic matter, the DIC increase is most likely of anthropogenic origin. The time trends agree reasonably well with C_{ant} changes in the inflowing waters of the NwAC and the WSC. As a result of the increases in DIC, the pH is reduced by 0.02–0.05 units during the last two decades. If these trends continue, the Atlantic layers of the Arctic Ocean will start to become undersaturated with respect to aragonite in less than 100 years. As extensive biological life occurs in this water, especially before entering the Arctic Ocean, this will have vital consequences for their living conditions.

The observed changes in primary production and specifically in the sedimentation of ice algae will most likely result in increased AOU, nutrients as well as DIC in the future. If the mean sedimentation rate of 9 g C m^{-2} [*Boetius et al*., 2013] is sustained annually and if most of it will decay and be added to the overlying water it can be observed within a short time. The resulting annual increase will if mixed within a 100 m thick layer be -9, 7, 1, and 0.1 μmol kg^{-1} in O_2, DIC, nitrate, and phosphate, respectively. However, it is highly unlikely that such a high spatial average sedimentation rate can be sustained by the supply of nutrients in the present Arctic Ocean.

Acknowledgments

We are grateful to K.-U. Ludwichowski and C. Burau for nutrient measurements and A. Wisotzki for oxygen probe calibration on board RV Polarstern in 2011. Measurements of DIC and TA during ARK-XXII2 were performed by S. Ober (NIOZ, Texel). The CO_2 data from Mount Zeppelin, Svalbard were provided by B. Noone and H.-C. Hansson, Department of Applied Environmental Science, Stockholm University. The atmospheric measurements are supported by the Swedish Environmental Protection Agency within its environmental monitoring program. Financial support was received from the Swedish Research Council (contract 621-2010-4084) and the European Union FP7 project CarboChange (under grant agreement 264879).

References

Anderson, L. G., E. P. Jones, and B. Rudels (1999), Ventilation of the Arctic Ocean estimated by a plume entrainment model constrained by CFCs, *J. Geophys. Res.*, *104*(C6), 13,423–13,429.

Anderson, L. G., E. P. Jones, and J. H. Swift (2003), Export production in the central Arctic Ocean evaluated from phosphate deficits, *J. Geophys. Res.*, *108*(C6), 3199, doi:10.1029/2001JC001057.

Anderson, L. G., E. Falck, E. P. Jones, S. Jutterström, and J. H. Swift (2004), Enhanced uptake of atmospheric CO_2 during freezing of seawater: A field study in Storfjorden, Svalbard, *J. Geophys. Res.*, *109*, C06004, doi:10.1029/2003JC002120.

Arrigo, K. R., and G. L. van Dijken (2011), Secular trends in Arctic Ocean net primary production, *J. Geophys. Res.*, *116*, C09011, doi:10.1029/2011JC007151.

Arrigo, K. R., P. A. Matrai, and G. L. van Dijken (2011), Primary productivity in the Arctic Ocean: Impacts of complex optical properties and subsurface chlorophyll maxima on large-scale estimates, *J. Geophys. Res.*, *116*, C11022, doi:10.1029/2011JC007273.

Årthun, M., R. B. Ingvaldsen, L. H. Smedsrud, and C. Schrum (2011), Dense water formation and circulation in the Barents Sea, *Deep Sea Res., Part I*, *58*, 801–817, doi:10.1016/j.dsr.2011.06.001.

Ballantyne, A. P., C. B. Alden, J. B. Miller, P. P. Tans, and J. W. C. White (2012), Increase in observed net carbon dioxide uptake by land and oceans during the past 50 years, *Nature*, *488*, 70–72, doi:10.1038/nature11299.

Bates, N. R., and J. T. Mathis (2009), The Arctic Ocean marine carbon cycle: Evaluation of air-sea CO_2 exchanges, ocean acidification impacts and potential feedbacks, *Biogeosciences*, *6*(11), 2433–2459.

Boetius, A., et al. (2013), Export of algal biomass from the melting Arctic sea ice, *Science*, *339*(6126), 1430–1432, doi:10.1126/science.1231346.

Bönisch, G., and P. Schlosser (1995), Deep water formation and exchange rates in the Greenland/Norwegian Sea and the Eurasian Basin of the Arctic Ocean derived from tracer data, *Prog. Oceanogr.*, *35*, 29–52.

Cai, P., M. R. van der Loeff, I. Stimac, E.-M. Nöthig, K. Lepore, and S. B. Moran (2010), Low export flux of particulate organic carbon in the central Arctic Ocean as revealed by ^{234}Th:^{238}U disequilibrium, *J. Geophys. Res.*, *115*, C10037, doi:10.1029/2009JC005595.

Clayton, T. D., and R. H. Byrne (1993), Spectrophotometric seawater pH measurements: Total hydrogen ion concentration scale calibration of *m*-cresol purple and at-sea results, *Deep Sea Res., Part I*, *40*(10), 2115–2129.

Codispoti, L. A., V. Kelly, A. Thessen, P. Matrai, S. Suttles, V. Hill, M. Steele, and B. Light (2013), Synthesis of primary production in the Arctic Ocean: III. Nitrate and phosphate based estimates of net community production, *Prog. Oceanogr.*, *110*, 126–150.

Dickson, A. G., and F. J. Millero (1987), A comparison of the equilibrium constants for the dissociation of carbonic acid in seawater media, *Deep Sea Res., Part A*, *34*(10), 1733–1743.

Dickson, A. G., C. L. Sabine, and J. R. Christian (Eds.) (2007), *Guide to Best Practices for Ocean CO_2 Measurements, PICES Special Publication*, vol. 3, 191 pp.

Else, B. G. T., T. N. Papakyriakou, R. J. Galley, W. M. Drennan, L. A. Miller, and H. Thomas (2011), Wintertime CO_2 fluxes in an Arctic polynya using eddy covariance: Evidence for enhanced air-sea gas transfer during ice formation, *J. Geophys. Res.*, *116*, C00G03, doi:10.1029/2010JC006760.

Gordon, L. I., J. C. Jennings, Jr., A. A. Ross, and J. M. Krest (1994), A suggested protocol for continuous flow automated analysis of seawater nutrients (phosphate, nitrate, nitrite and silicic acid) in the WOCE Hydrographic Program and the Joint Global Ocean Fluxes Study, in *WOCE Operations Manual*, WHP Off. Rep. WHPO 91-1, WOCE Rep. 68/91, rev. 1, Woods Hole, Mass.

Haraldsson, C., L. G. Anderson, M. Hassellöv, S. Hulth, and K. Olsson (1997), Rapid, high-precision potentiometric titration of alkalinity in ocean and sediment pore waters, *Deep Sea Res., Part I*, *44*(12), 2031–2044.

Harms, I. H. (1997), Water mass transformation in the Barents Sea—Application of the Hamburg Shelf Ocean Model (HamSOM), *ICES J. Mar. Sci.*, *54*, 351–365.

Jakobsson, M., J. Backman, A. Murray, and R. Løvlie (2003), Optically Stimulated Luminescence dating supports central Arctic Ocean cm-scale sedimentation rates, *Geochem. Geophys. Geosyst.*, *4*, 1016, doi:10.1029/2002GC000423.

Johansson, O., and M. Wedborg (1982), On the evaluation of potentiometric titrations of sea-water with hydrochloric-acid, *Oceanol. Acta*, *5*(2), 209–218.

Johnson, K. M., J. M. Sieburth, P. J. L. Williams, and L. Brändström (1987), Coulometric total carbon dioxide analysis for marine studies: Automation and calibration, *Mar. Chem.*, *21*, 117–133.

Jones, E. P., B. Rudels, and L. G. Anderson (1995), Deep waters of the Arctic Ocean: Origins and circulation, *Deep Sea Res., Part I*, *42*, 737–760.

Jutterström, S., and L. G. Anderson (2005), The saturation of calcite and aragonite in the Arctic Ocean, *Mar. Chem.*, *94*, 101–110.

Jutterström, S., and L. G. Anderson (2010), Uptake of CO_2 by the Arctic Ocean in a changing climate, *Mar. Chem.*, *122*, 96–104, doi:10.1016/j.marchem.2010.07.002.

Jutterström, S., L. G. Anderson, N. R. Bates, R. Bellerby, T. Johannessen, E. P. Jones, R. M. Key, X. Lin, A. Olsen, and A. M. Omar (2010), Arctic Ocean data in CARINA, *Earth Sys. Sci. Data*, *2*, 71–78.

Key, R. M., T. Tanhua, A. Olsen, M. Hoppema, S. Jutterström, C. Schirnick, S. van Heuven, A. Kozyr, X. Lin, A. Velo, D. W. R. Wallace, and L. Mintrop (2010), The CARINA data synthesis project: Introduction and overview, *Earth Sys. Sci. Data*, *2*, 105–121.

Korhonen, M., B. Rudels, M. Marnela, A. Wisotzki, and J. Zhao (2012), Time and space variability of freshwater content, heat content and seasonal ice melt in the Arctic Ocean from 1991 to 2011, *Ocean Sci. Discuss.*, *9*, 2621–2677, doi:10.5194/osd-9–2621-2012.

Laxon, S. W., et al. (2013), CryoSat-2 estimates of Arctic sea ice thickness and volume, *Geophys. Res. Lett.*, *40*, 732–737, doi:10.1002/grl.50193.

Lenton, A., N. Metzl, T. Takahashi, M. Kuchinke, R. J. Matear, T. Roy, S. C. Sutherland, C. Sweeney, and B. Tilbrook (2012), The observed evolution of oceanic pCO_2 and its drivers over the last two decades, *Global Biogeochem. Cycles*, *26*, GB2021, doi:10.1029/2011GB004095.

Le Quéré, C., et al. (2009), Trends in the sources and sinks of carbon dioxide, *Nat. Geosci.*, *2*, 831–836, doi:10.1038/ngeo689.

Li, W. K. W., F. A. McLaughlin, C. Lovejoy, and E. C. Carmack (2009), Smallest algae thrive as the Arctic Ocean freshens, *Science*, *326*(5952), 539, doi:10.1126/science.1179798.

Marnela, M., B. Rudels, K. A. Olsson, L. G. Anderson, E. Jeansson, D. J. Torres, M.-J. Messias, J. H. Swift, and A. J. Watson (2008), Transports of Nordic Seas water masses and excess SF_6 through Fram Strait to the Arctic Ocean, *Prog. Oceanogr.*, *78*, 1–11, doi:10.1016/j.pocean.2007.06.004.

Mauritzen, C. (1996), Production of dense overflow waters feeding the North Atlantic across the Greenland-Scotland Ridge. Part 1: Evidence for a revised circulation scheme, *Deep Sea Res., Part I*, *43*(6), 769–806, doi:10.1016/0967-0637(96)00037-4.

Mehrbach, C., C. H. Culberson, J. E. Hawley, and R. M. Pytkowicz (1973), Measurement of the apparent dissociation constants of carbonic acid in seawater at atmospheric pressure, *Limnol. Oceanogr.*, *18*(6), 897–907.

Mintrop, L., F. F. Perez, M. Gonzalez-Davila, M. J. Santana-Casiano, and A. Kortzinger (2000), Alkalinity determination by potentiometry: Intercalibration using three different methods, *Cienc. Mar.* *26*(1), 23–37.

Olsen, A., et al. (2006), Magnitude and origin of the anthropogenic CO_2 increase and ^{13}C Suess effect in the Nordic seas since 1981, *Global Biogeochem. Cycles*, *20*, GB3027, doi:10.1029/2005GB002669.

Omar, A. M., T. Johannessen, S. Kaltin, and A. Olsen (2003), Anthropogenic increase of oceanic pCO_2 in the Barents Sea surface water, *J. Geophys. Res.*, *108*(C12), 3388, doi:10.1029/2002JC001628.

Omar, A. M., T. Johannessen, R. G. J. Bellerby, A. Olsen, S. Kaltin, C. Kivimae, and L. G. Anderson (2005), Sea ice and brine formation in Storfjorden: Implications for the uptake of atmospheric CO_2 in future Arctic Ocean, in *The Nordic Seas: An Integrated Perspective, AGU Monogr. Ser.*, vol. 158, edited by H. Drange et al., pp. 177–188, AGU, Washington, D. C.

Polyakov, I. V., et al. (2010), Arctic Ocean warming contributes to reduced polar ice cap, *J. Phys. Oceanogr.*, *40*, 2743–2756, doi:10.1175/2010JPO4339.1.

Redfield, A. C., B. H. Ketchum, and F. A. Richards (1963), The influence of organisms on the composition of sea-water, in *The Sea: Ideas and Observations on the Progress in the Study of the Seas*, vol. 2, edited by M. N. Hill, pp. 26–77, Interscience, New York.

Revelle, R. (1983), The oceans and the carbon dioxide problem, *Oceanus*, *26*, 3–9.

Riebesell, U., K. G. Schulz, R. G. J. Bellerby, M. Botros, P. Fritsche, M. Meyerhöfer, C. Neill, G. Nondal, A. Oschlies, J. Wohlers, and E. Zöllner (2007), Enhanced biological carbon consumption in a high CO_2 ocean, *Nature*, *450*, 545–548, doi:10.1038/nature062672007.

Rudels, B., L. G. Anderson, and E. P. Jones (1996), Formation and evolution of the surface mixed layer and halocline of the Arctic Ocean, *J. Geophys. Res.*, *101*(C4), 8807–8821.

Rudels, B., G. Björk, J. Nilsson, P. Winsor, I. Lake, and C. Nohr (2005), The interaction between waters from the Arctic Ocean and the Nordic Seas north of Fram Strait and along the East Greenland Current: Results from the Arctic Ocean-02 Oden expedition, *J. Mar. Syst.*, *55*, 1–30, doi:10.1016/j.jmarsys.2004.06.00.

Rudels, B., L. G. Anderson, P. Eriksson, E. Fahrback, M. Jakobsson, E. P. Jones, H. Melling, S. Prinsenberg, U. Schauer, and T. Yao (2012a), Observations in the ocean, in *Arctic Climate Change: The ACSYS Decade and Beyond, Atmos. Oceanogr. Sci. Libr.*, vol. 43, edited by P. Lemke and H.-W. Jacobi, pp. 117–198, doi:10.1007/978-94-007–2027-5_4. © Springer Science + Business Media B.V., pp. 117–198.

Rudels, B., M. Korhonen, G. Budéus, A. Beszczynska-Möller, U. Schauer, A. Nummelin, D. Quadfasel, and H. Valdimarsson (2012b), The East Greenland Current and its impacts on the Nordic Seas: Observed trends in the past decade, *ICES J. Mar. Sci.*, *69*, 841–851.

Rudels, B., U. Schauer, G. Björk, M. Korhonen, S. Pisarev, B. Rabe, and A. Wisotzki (2013), Observations of water masses and circulation with focus on the Eurasian Basin of the Arctic Ocean from the 1990s to the late 2000s, *Ocean Sci.*, *9*, 147–169, doi:10.5194/os-9–147-2013.

Rysgaard, S., J. Bendtsen, B. Delille, G. S. Dieckmann, R. N. Glud, H. Kennedy, J. Mortensen, S. Papadimitriou, D. N. Thomas, and J.-L. Tison (2011), Sea ice contribution to the air-sea CO_2 exchange in the Arctic and Southern Oceans, *Tellus, Ser. B*, *63B*, 823–830, doi:10.1111/j.1600-0889.2011.00571.x.

Sabine, C. L., R. A. Feely, F. J. Millero, A. G. Dickson, C. Langdon, S. Mecking, and D. Greeley (2008), Decadal changes in Pacific carbon, *J. Geophys. Res.*, *113*, C07021, doi:10.1029/2007JC004577.

Schauer, U., B. Rudels, E. P. Jones, L. G. Anderson, R. D. Muench, G. Björk, J. H. Swift, V. Ivanov, and A.-M. Larsson (2002), Confluence and redistribution of Atlantic water in the Nansen, Amundsen and Makarov basins, *Ann. Geophys.*, *20*, 257–273, doi:10.5194/angeo-20–257-2002.

Schuster, U., A. J. Watson, N. R. Bates, A. Corbiere, M. Gonzalez-Davila, N. Metzl, D. Pierrot, and M. Santana-Casiano (2009), Trends in North Atlantic sea-surface fCO_2 from 1990 to 2006, *Deep Sea Res., Part II*, *56*, 620–629, doi:10.1016/j.dsr2.2008.12.011.

Serreze, M. C., and J. A. Francis (2006), The Arctic amplification debate, *Clim. Change*, *76*, 241–264, doi:10.1007/s10584-005-9017-y.

Skjelvan, I., E. Falck, F. Rey, and S. B. Kringstad (2008), Inorganic carbon time series at Ocean Weather Station M in the Norwegian Sea, *Biogeosciences*, *5*, 549–560.

Stroeve, J., M. M. Holland, W. Meier, T. Scambos, and M. Serreze (2007), Arctic sea ice decline: Faster than forecast, *Geophys. Res. Lett.*, *34*, L09501, doi:10.1029/2007GL029703.

Stroeve, J. C., M. C. Serreze, M. M. Holland, J. E. Kay, J. Malanik, and A. P. Barrett (2012), The Arctic's rapidly shrinking sea ice cover: A research synthesis, *Clim. Change*, *110*, 1005–1027, doi:10.1007/s10584-011-0101-1.

Tanhua, T., E. P. Jones, E. Jeansson, S. Jutterström, W. M. Smethie Jr., D. W. R. Wallace, and L. G. Anderson (2009), Ventilation of the Arctic Ocean: Mean ages and inventories of anthropogenic CO_2 and CFC-11, *J. Geophys. Res.*, *114*, C01002, doi:10.1029/2008JC004868.

Tremblay, J.-É., and J. Gagnon (2009), The effects of irradiance and nutrient supply on the productivity of Arctic waters: A perspective on climate change, in *Influence of Climate Change on the Changing Arctic and Sub-Arctic Conditions*, edited by J. C. J. Nihoul and A. G. Kostianoy, pp. 73–93, Springer, New York.

Tsubouchi, T., S. Bacon, A. C. Naveira Garabato, Y. Aksenov, S. W. Laxon, E. Fahrbach, A. Beszczynska-Möller, E. Hansen, C. M. Lee, and R. B. Ingvaldsen (2012), The Arctic Ocean in summer: A quasi-synoptic inverse estimate of boundary fluxes and water mass transformation, *J. Geophys. Res.*, *117*, C01024, doi:10.1029/2011JC007174.

van Heuven, S., D. Pierrot, J. W. B. Rae, E. Lewis, and D. W. R. Wallace (2011), MATLAB program developed for CO2 system calculations, *Rep. ORNL/CDIAC-105b*, Carbon Dioxide Inf. Anal. Cent., Oak Ridge, Tenn., doi:10.3334/CDIAC/otg.CO2SYS_MATLAB_v1.1.